PHYSICAL REVIEW B VOLUME 34, NUMBER 8 15 OCTOBER 1986

Numerical and analytic methods for the study of disordered alloy surfaces

X. Zhang, M. Hwang, A. Gonis, and A. J. Freeman
Department of Physics and Astronomy, Northwestern University, Evanston, Illinois 60201

(Received 18 February 1986)

We report exact, numerically simulated, and analytic calculations of the density of states (DOS) at or near the surface of semi-infinite substitutionally disordered alloys in the tight-binding approximation to the Hamiltonian. The exact DOS is obtained through a recursion method, which is applicable to systems of any dimensionality, and yields results which possess the desirable analytic and convergence properties. Both the surface generalization of the coherent-potential approximation (CPA) and of the embedded-cluster method (ECM) are used to calculate averaged and partial DOS's and to compare them with the exact results. As is the case with bulk alloys, the CPA yields a smooth overall description of the exact spectra, while the ECM properly reproduces much of the structure of the DOS even when used with relatively small clusters of atoms. A discussion of the work and its possible utility is given.

I. INTRODUCTION

In this paper we present an exact numerical technique as well as analytic methods for the calculation of the density of states (DOS) on the surfaces of substitutionally disordered alloys described by tight-binding (TB) Hamiltonians. The methods presented here are applicable to the study of the surfaces of two- as well as three-dimensional materials and are thus an extension of some of our previous work[1] on semi-infinite, one-dimensional disordered systems.

The importance of understanding the properties of semi-infinite ordered and substitutionally disordered materials has led to the development of a large number[2–12] of approaches for the study of surfaces within various physical models and formalisms. In our study[1] of concentrated, substitutionally disordered semi-infinite chains we used the position-space renormalization-group (PSRG) method[13–15] (also called the decimation technique) to obtain "exact," numerically simulated, electronic DOS's at or near one-dimensional surfaces. The PSRG method can be formally generalized to two- and three-dimensional semi-infinite materials but its implementation becomes computationally very difficult with increasing dimensionality. On the other hand, the recursion algorithm presented in Sec. II is computationally simple enough to provide a viable technique for the study of surfaces of two- and three-dimensional disordered systems. The numerical calculations for the electronic DOS on the surface of a substitutionally disordered alloy based on a two-dimensional square lattice presented here indicate the viability of the method and demonstrate that this numerical algorithm converges sufficiently rapidly so that stable and reliable results can be obtained with samples containing only moderately large ($\sim 10^4$) numbers of sites.

In our study[1] of one-dimensional semi-infinite disordered systems we also investigated several analytic methods for calculating the DOS at or near substitutionally disordered surfaces. One of these methods made use of the continued-fraction expansion[16] in conjunction with the augmented space formalism,[17,18] and yielded results which were in rough agreement with the DOS determined by the exact PSRG method but missed most of the detailed structure of the latter. By contrast the embedded-cluster method[1,19,20] (ECM) was found to reproduce the features of the exact spectra even with clusters of moderate size (7–13 atoms).

In this paper we use two analytic techniques for the calculation of the single-particle spectra on the surface of substitutionally disordered alloys. One of these methods is a generalization[8] of the coherent-potential approximation[21–26] (CPA) for bulk disordered materials to alloy surfaces, and the other is a similar extension of the ECM. We now give a brief description of both of these methods.

The CPA (Refs. 21–26) has proved to be the most reliable and accurate single-site theory for the study of bulk, substitutionally disordered alloys. In the CPA, one considers the real, disordered material as replaced by an effective medium characterized by an energy-dependent, complex site potential (self-energy). This potential is determined by the self-consistency condition that the scattering resulting from a real atom embedded in the medium vanishes upon averaging over all alloy constituents. As a result the CPA accounts properly for statistical fluctuations confined to a single site, and has a large number of physically and mathematically desirable properties. Thus, the CPA always yields analytic,[27] physically meaningful results, e.g., non-negative DOS, has the proper behavior in the limits of vanishing scattering strength or concentration and constitutes a proper interpolation scheme away from those limits.[23,24] In spite of these desirable properties, however, the CPA cannot account for statistical fluctuations extending beyond a single site and thus cannot be used properly in the study of many physical properties, e.g., short-range order, formation of magnetic moments, etc., in which local environment fluctuations play a significant role. Local environment effects can only be taken accurately into account within a multisite or cluster theory.

Of the many cluster methods[28–29] (of which we cite only a small, representative sample) which have been proposed for the treatment of local environment effects, the ECM (Refs. 19 and 20) has proved to be the most useful. Although the ECM introduces no further self-consistency than that already embodied in the CPA, it preserves the analytic properties of the latter and allows the proper treatment of local statistical fluctuations associated with compact clusters of atoms in the material. In fact, regardless of the method used to determine the effective medium, be that method the CPA, the molecular CPA,[28] the traveling cluster approximation,[37] or any other technique, it can easily be confirmed that the ECM is essential in the treatment of *arbitrary* clusters of atoms embedded in that medium. This approach, the treatment of small clusters of atoms surrounded by a properly chosen analytic effective medium, has been shown to yield accurate results for the single-particle, e.g., DOS's, and two-particle,[40] e.g., ac conductivity, properties of substitutionally disordered bulk alloys. In this paper it is shown that the ECM can be generalized in a straightforward way to the study of surface properties of substitutionally disordered two- and three-dimensional materials.

The development of analytic theories for substitutionally disordered systems has profitted greatly from comparisons between the result of calculations based on such theories and exact or experimental results, where such were available. It was particularly the comparison with exact computer simulations for model tight-binding systems obtained primarily through the use of the negative eigenvalue theorem[41] which aided in sorting out various approximations on the basis of accuracy, analytic properties, and ease of computation. The negative eigenvalue theorem, however, is inapplicable to semi-infinite materials. In contrast, both the PSRG method and the recursion algorithm to be presented here can be used in the study of infinite as well as semi-infinite disordered solids. The results and comparisons presented in this paper provide a link between analytic theories, such as the CPA and the ECM, and exact methods for the study of disordered surfaces. They are also a guide to the further development of approximate methods for the study of materials lacking full three-dimensional character, as corresponding comparisons have been in regard to three-dimensional, infinite systems.

The remainder of the paper is arranged as follows. In Sec. II we present our numerical algorithm for calculating the DOS's on the surface of two- and three-dimensional substitutionally disordered alloys. The generalizations of the CPA and the ECM to the study of alloy surfaces are given in Sec. III. In Sec. IV we present the results and comparisons of calculations based on these formalisms, while Sec. V contains a discussion of our work and certain conclusions which can be drawn from it.

II. THE RECURSION ALGORITHM

The recursion algorithm[42] is most easily adaptable to systems described by Hamiltonians of a TB character. Thus, we consider a binary alloy, A_cB_{1-c}, characterized by a single-band model Hamiltonian of the well-known form

$$H=\sum_{i}\varepsilon_i\,|i\rangle\langle i|+\sum_{\substack{i>j\\ i,j}}W_{ij}(\,|i\rangle\langle j|+|j\rangle\langle i|\,)\ . \tag{2.1}$$

Here, ε_i can assume the "values" ε_A or ε_B with corresponding probability c or $1-c$, depending on whether site i is occupied by an atom of type A or B, respectively. The hopping integral, W_{ij}, in general depends on the occupation of sites i and j, a dependence referred to as off-diagonal disorder (ODD). For simplicity, in our calculations we consider only diagonal disorder with W_{ij} depending only on the distance between sites i and j. The effects of ODD as well as those of multiple bands and polyatomic unit cells can be included in the computation in a straightforward way but with a certain increase in computational labor.

The essential idea of the recursion technique can best be presented with reference to a one-dimensional disordered chain of $N+1$ sites. The Hamiltonian of such a chain can be written in the form

$$H^{(N+1)}=H_0+H'\ , \tag{2.2}$$

where

$$H_0=H^{(N)}+\varepsilon_{N+1}\,|N+1\rangle\langle N+1| \tag{2.3}$$

is the Hamiltonian describing the coupled first N sites and the "decoupled" $(N+1)$th site. Thus, $H^{(N)}$ has the form of Eq. (2.1),

$$H^{(N)}=\sum_{i=1}^{N}\varepsilon_i\,|i\rangle\langle i|+\sum_{i=1}^{N-1}W(\,|i\rangle\langle i+1|+|i+1\rangle\langle i|\,)\ , \tag{2.4}$$

with the hopping, W, restricted to nearest neighbors for simplicity. Now, the "perturbation" H' in Eq. (2.2) is the coupling between the $(N+1)$th site and the Nth site,

$$H'=W(\,|N\rangle\langle N+1|+|N+1\rangle\langle N|\,)\ . \tag{2.5}$$

The Green's function corresponding to $H^{(N+1)}$ can then be determined from the Dyson equation,

$$G^{(N+1)}=G_0+G_0H'G^{(N+1)}\ , \tag{2.6}$$

where the unperturbed resolvent corresponding to H_0 is given by the expression

$$G_0(z)=G^{(N)}+\,|N+1\rangle(z-\varepsilon_{N+1})^{-1}\langle N+1|\ , \tag{2.7}$$

with z a complex energy parameter, $z=E+i\eta$, where E is real and η is an infinitesimal positive part. Equations (2.6) and (2.7) allow the implementation of a recursive procedure for determining $G^{(N+1)}$. Since the $(N+1)$th site couples only to the Nth site, the one-electron Green function at the boundary site can be calculated by the recursive expression

$$G^{(N+1)}_{N+1,N+1}=(z-\varepsilon_{N+1}-W^2G^{(N)}_{N,N})^{-1} \tag{2.8}$$

for the $(N+1,N+1)$ matrix elements of $G^{(N+1)}$ in terms of the (N,N) matrix element of $G^{(N)}$. The element $G^{(N)}_{N,N}$ can also be expressed by means of an equation such as Eq. (2.8) which leads to a solution for $G^{(N+1)}_{N+1,N+1}$. Finally, the local density of states at the boundary site $N+1$ is given by the usual expression

$$n^{(N+1)}(z) = -\frac{1}{\pi}\,\mathrm{Im}G^{(N+1)}_{N+1,N+1}(z)\ . \tag{2.9}$$

The prescription outlined thus far is valid only for one-dimensional systems. However, the form of Eq. (2.8) is preserved in applications to two- and three-dimensional finite-size systems by an appropriate redefinition of the scalar quantities entering Eq. (2.8) as matrices. Let us consider a rectangular section of a square lattice with $N_1 \times N_2$ sites, shown schematically in Fig. 1. We consider the lattice as a collection of N_2 linear molecules or clusters of N_1 sites each as is indicated by the dotted lines in Fig. 1. The cluster energy, hopping terms, and Green function matrix elements are now $N_1 \times N_1$ matrices in the cluster space, and Eq. (2.8) assumes the form

$$\underline{G}^{(N+1)}_{N+1,N+1} = (z\underline{I} - \underline{\epsilon}_{N+1} - \underline{W}\,\underline{G}^{(N)}_{N,N}\underline{W})^{-1}\ , \tag{2.10}$$

where the subscripts N and $N+1$ refer to clusters and the underlines denote $N_1 \times N_1$ matrices with $\underline{I}$ being the unit matrix.

The recursive process generated by Eq. (2.10) can be outlined as follows.

(i) Initialize $\underline{G}^{(0)}_{0,0}$, i.e.,

$$\underline{G}^{(0)}_{0,0} = \underline{0}\ . \tag{2.11a}$$

(ii) Generate the $(N+1)$th line with the parameters corresponding to the disordered material under consideration and obtain $\underline{G}^{(N+1)}_{N+1,N+1}$ using Eq. (2.10).

(iii) Calculate the density of states from the expression

$$n^{(N+1)}(z) = -\frac{1}{\pi}\frac{1}{N_1}\mathrm{Im}\,\mathrm{Tr}\underline{G}^{(N+1)}_{N+1,N+1}(z)\ , \tag{2.11b}$$

where $n^{(N+1)}(z)$ is the average density of states of the $(N+1)$th line which, by construction, is a boundary of the iterated lattice, i.e., the lattice with $N_1 \times (N+1)$ sites.

(iv) Repeat steps (ii) and (iii) until the desired sample size is reached.

(v) Perform the average,

$$n(z) = \frac{1}{N_2}\sum_{i=N_0}^{N_0+N_2-1} n^{(i)}(z)\ , \tag{2.12}$$

where the first N_0 lines are truncated (neglected) in order to minimize the effects associated with our use of samples of finite size. Clearly, these considerations can be generalized to three-dimensional systems in a straightforward way.

The advantage of the algorithm just described in comparison to a straightforward use of the PSRG decimation method is that it requires comparatively small memory since only $\underline{G}^{(N)}_{N,N}$ needs to be stored at each step. This allows simulations with rather large samples. We point out that, for the sake of simplicity, the averaged DOS at the $(N+1)$th line is calculated from the trace of $\underline{G}^{(N+1)}_{N+1,N+1}$, which effectively implies that we neglect the effects of the boundary sites on the line. For moderately large-size clusters such effects can safely be ignored.

The recursive algorithm used here is a generalization to disordered surfaces of the transfer matrix method[5] used to study the electronic structure of ordered (translationally invariant) semi-infinite solids within the TB approximation. In the latter case, the methods become identical. Real-space methods, however, are necessary in order to treat disordered surfaces for which the concept of Fourier transformation is, strictly speaking, inapplicable.

The application of the present method to three-dimensional surfaces apparently requires the use of rather large matrices, of order N^2, where N is the number of the lattice points on the surface plane. Use of present-day supercomputers can easily accommodate values of N sufficiently large for our purposes (of the order of 50). In fact, the value of N necessary to obtain converged results decreases with increasing disorder reflecting the corresponding decrease in the electronic mean-free path. Thus, realistic three-dimensional calculations can be carried out without too great a difficulty in the majority of cases.

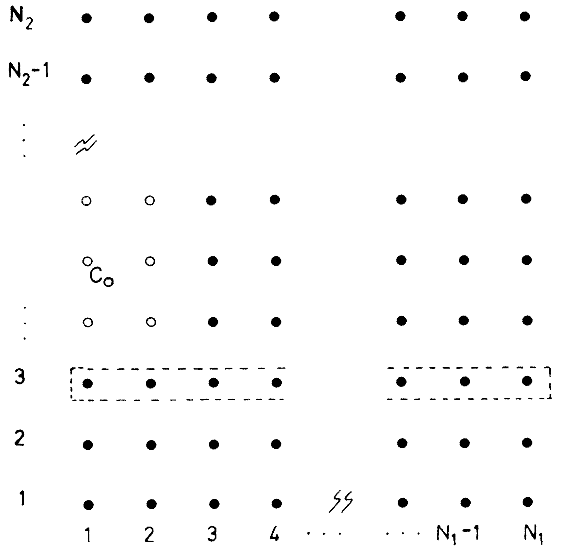

FIG. 1. Schematic diagram of a square lattice with $N_1 \times N_2$ sites. The dotted lines identify a one-dimensional molecule or cluster of N_1 sites. The open circles indicate the cluster used in applications of the ECM discussed in the text, with C_0 denoting the center of the cluster.

III. THE CPA AND THE ECM FOR SUBSTITUTIONALLY DISORDERED SURFACES

In this section we present a summary version of the extension of the CPA to alloy surfaces as proposed by Berk[8] and also describe the extension of the ECM to substitutionally disordered semi-infinite systems.

A. CPA for surfaces of substitutionally disordered alloys

For the sake of simplicity of presentation, we consider the case of simple semi-infinite lattices which can be thought of as being generated by the repetition in one direction of a basic plane. More complicated structures consisting of the repetition of a stack of planes can be treated in a straightforward generalization of the methods presented below. Furthermore, we consider the case of unrelaxed disordered surfaces in which the potential on planes near or on the surface, and the concentrations of the various species and the crystal structure are identical to those characterizing the bulk alloy. Finally, we will focus our discussion on diagonally disordered single-band binary alloys as described in Sec. II. All of these restrictions can be removed in a conceptually simple manner but with a concomital increase in computational labor.

For the discussion of surface properties it is convenient to label the matrix elements of the Hamiltonian, Eq. (2.1), by the planes, $I_0, I_1, \ldots$, etc., parallel to the surface and the sites, $i,j,\ldots$, etc., belonging to these planes. In our notation, the surface plane is labeled by I_0. Thus, the TB single-band Hamiltonian of Eq. (2.1) can be written in the form

$$\begin{aligned} H = & \sum_{I,i} \varepsilon_i^I \,|I,i\rangle\langle I,i| \\ & + \sum_{\substack{i,j\\ I,J}} W_{ij}^{IJ} (\,|I,i\rangle\langle J,j| + |J,j\rangle\langle I,i)|\,)\,, \end{aligned} \tag{3.1}$$

where $W_{I_i,I_i} \equiv 0$. The Green function is given by usual expression

$$G(z) = (z - H)^{-1}\,, \tag{3.2}$$

and the local DOS associated with site i in plane I is obtained from the average

$$n_i^I(E) = -\frac{1}{\pi}\,\mathrm{Im}\langle G_{ii}^{II}(E)\rangle_{(i)}\,, \tag{3.3}$$

where the symbol $\langle \cdots \rangle_{(i)}$ denotes an average over all alloy configurations in which the occupation of site i remains fixed. We use the notation $\langle \cdots \rangle$ without subscripts to denote an average over all configurations including the occupation of site i.

Clearly, an exact evaluation of the average in Eq. (3.3) is an impossible task and this average must be evaluated in an approximate fashion. In the spirit of the CPA, we consider the semi-infinite disordered material replaced with an "ordered" medium characterized by plane self-energies σ^I, and an effective Hamiltonian

$$\begin{aligned} \overline{H} = & \sum_{I,i} \sigma^I \,|I,i\rangle\langle I,i| \\ & + \sum_{\substack{i,j\\ I,J}} W_{ij}^{IJ} (\,|I,i\rangle\langle J,j| + |J,j\rangle\langle I,i|\,) \end{aligned} \tag{3.4}$$

in which the W_{ij}^{IJ} are identical to the quantities occurring in Eq. (3.1). The last expression can be cast into a convenient form through a Fourier transform (FT) in a direction parallel to the surface. We introduce a mixed Bloch-Wannier representation[4] in which a quantity $A(\mathbf{x},\mathbf{y})$ can be represented in the form

$$A(\mathbf{x},\mathbf{k}_y) = \frac{1}{N_y}\int d^2y\, A(\mathbf{x},\mathbf{y})\, e^{i\mathbf{k}_y\cdot\mathbf{y}}\,, \tag{3.5}$$

where N_y is the number of values taken by the variable y ($\mathbf{x}$ and $\mathbf{y}$ assumed discrete). In this representation, the FT of the intraplanar hopping integral, W_{ij}^{II}, i and j belonging to plane I, is given by the expression

$$W^{II}(\mathbf{k}_{\parallel}) = \frac{1}{N_I^2}\sum_{\substack{i,j\\ i\neq j}} W_{ij}^{II} e^{i\mathbf{k}_{\parallel}\cdot(\mathbf{R}_i-\mathbf{R}_j)}\,, \tag{3.6}$$

where $\mathbf{k}_{\parallel}$ is a vector parallel to the surface and belonging to the first Brillouin zone defined by the structure of the surface,[4] while $\mathbf{R}_i$ and $\mathbf{R}_j$ denote the positions of sites in planes parallel to the surface. Finally, N_I denotes the number of sites in plane I (which for the model considered here is independent of I). Similarly the interplanar hopping can be written in the form

$$W^{IJ}(\mathbf{k}_{\parallel}) = \frac{1}{N_I N_J}\sum_{\substack{i\in I\\ j\in J}} W_{ij}^{IJ} e^{i\mathbf{k}_{\parallel}\cdot(\mathbf{R}_i-\mathbf{R}_j)}\,, \quad I\neq J \tag{3.7}$$

where $i \in I$ indicates that site i belongs to plane I. Using Eqs. (3.6) and (3.7), we can write the effective Hamiltonian, Eq. (3.4), in the form

$$\begin{aligned} \overline{H}(\mathbf{k}_{\parallel}) = & \sum_{I} \sigma^I \,|I\rangle\langle I| \\ & + \sum_{I,J} W^{IJ}(\mathbf{k}_{\parallel}) (\,|I\rangle\langle J| + |J\rangle\langle I|\,)\,, \\ & I,J = 0,1,2,\ldots \end{aligned} \tag{3.8}$$

with a corresponding Green function

$$G^{IJ}(z;\mathbf{k}_{\parallel}) = \{[z - \overline{H}(\mathbf{k}_{\parallel})]^{-1}\}_{I,J}\,. \tag{3.9}$$

We emphasize that $\overline{H}(\mathbf{k}_{\parallel})$ is a function of the complex energy variable z through the corresponding dependence of the self-energies, $\sigma^I(z)$. Also, it is clear that Eq. (3.8) is formally identical to that for a one-dimensional semi-infinite system with "site" energies σ^I, and "intersite" hopping $W^{IJ}(\mathbf{k}_{\parallel})$. The matrix elements $\overline{G}_{ij}^{IJ}(z)$ for a site i in plane I and a site j in plane J are obtained by the inverse FT

$$G_{ij}^{IJ}(z) = \frac{1}{N_{\parallel}}\sum_{\mathbf{k}_{\parallel}} G^{IJ}(\mathbf{k}_{\parallel}) e^{-i\mathbf{k}_{\parallel}\cdot(\mathbf{R}_i-\mathbf{R}_j)}\,. \tag{3.10}$$

It now remains to provide a prescription for determining the still unknown self-energies σ^I. In the spirit of the CPA we impose the conditions

$$\langle t_{ii}^{II}\rangle = 0 \tag{3.11a}$$

for the plane scattering matrix, or

$$\langle G_{ii}^{II}(z)\rangle = \overline{G}_{ii}^{II} \tag{3.11b}$$

for the corresponding Green function, where the average is over the occupation of a single site. Explicitly we can write these conditions in the respective forms,

$$\langle t_{ii}^{II}\rangle = \langle(\varepsilon_i^I - \sigma^I)/[1 - (\varepsilon_i^I - \sigma^I)\overline{G}^{II}]\rangle \tag{3.12a}$$

and

$$\overline{G}^{II} = \langle[\sigma^I - \varepsilon_i^I + (\overline{G}^{II})^{-1}]^{-1}\rangle\,, \tag{3.12b}$$

corresponding to Eqs. (3.11a) and (3.11b), with $G^{II} = G_{ii}^{II}$. In these equations G_{ii}^{II} denotes the Green function associated with a real atom at site i in plane I embedded in an effective medium obtained in the CPA. Since $\overline{G}^{II}$ is a function of *all* σ^J, these conditions constitute an infinite system of coupled equations for determining the self-energies σ^I at each energy of interest.

In order to solve the set of equations represented by the self-consistency conditions [(3.12a) and (3.12b)], we use the observation that σ^I as a local quantity must converge toward a limiting value, σ^b, b denoting bulk for I far away from the surface,

$$\sigma^I \rightarrow \sigma^b \text{ as } I \rightarrow \infty \ . \tag{3.13}$$

Therefore, we can truncate the set of equations [(3.13), (3.12a), and (3.12b)] after a conveniently chosen value of I, $I_{\max}$, replacing all σ^I for $I \geq I_{\max}$ with σ^b. The results of numerical calculations presented in Sec. IV show that σ^I converges sufficiently strongly to its limiting value σ^b so that $I_{\max}$ can be chosen as relatively small, say, $I_{\max}=2$ or 3.

B. Computational considerations

In this subsection, we exhibit in some detail the structure of Eqs. (3.12b) thus clarifying somewhat the computational aspects of their solution. We note that the bulk Green function, G^b, for the alloy in the CPA can be obtained from the Dyson equation

$$\begin{aligned}\bar{G}^b(\mathbf{k}_\|)&=g^b(\mathbf{k}_\|)+g^b(\mathbf{k}_\|)\Delta(\mathbf{k}_\|)\bar{G}^b(\mathbf{k}_\|)\\&=[g^b(\mathbf{k}_\|)^{-1}-\Delta(\mathbf{k}_\|)]^{-1} \ .\end{aligned} \tag{3.14}$$

Here,

$$g^b(\mathbf{k}_\|)=[z-\sigma^b-W^0(\mathbf{k}_\|)]^{-1} \tag{3.15}$$

is the Green's function of a single plane in the bulk alloy, with $W^0(\mathbf{k}_\|)$ defined in Eq. (3.6) being the FT of the intraplanar hopping, and $\Delta(\mathbf{k}_\|)$ is the renormalized interactor[19] (RI) describing the interaction of any plane with the rest of the bulk material. The RI can be obtained from Eq. (3.14) for any energy, z, and wave vector $\mathbf{k}_\|$, in the form

$$\Delta(\mathbf{k}_\|)=[z-\sigma^b-W^0(\mathbf{k}_\|)]-[G^b(\mathbf{k}_\|)]^{-1} \tag{3.16}$$

once $\bar{G}^b(\mathbf{k}_\|)$ has been determined. As a simple example consider the case in which the hopping W is confined to near neighbors. Then, the Green's function $G^{II}(\mathbf{k}_\|)$ for any plane I in the semi-infinite material can be written in a convenient continued-fraction form. In particular, imposing the "surface-bulk" approximation, i.e., $I_{\max}=0$, with only the surface described by a self-energy different from that of the bulk, we obtain for the surface Green function the expression

$$G^{00}(\mathbf{k}_\|)=\left[z-\sigma^0-W^0(\mathbf{k}_\|)-\frac{\Delta(\mathbf{k}_\|)}{2}\right]^{-1} , \tag{3.17}$$

where $\Delta(\mathbf{k}_\|)/2$ denotes the interaction of the surface plane with half of the bulk material on one side. In this case only σ^0 is to be determined and conditions (3.12) reduce to a single equation.

C. Embedded-cluster method (ECM) for surfaces

As has been shown in previous work,[19,20] the ECM constitutes the simplest cluster theory based on the CPA that yields physically meaningful, accurate results in most cases of physical interest. In the ECM, one calculates exactly the Green function of a cluster of atoms embedded in a given translationally invariant medium such as that obtained in the CPA. The cluster Green function takes the form

$$\underline{G}^c(z)=[z\underline{I}-\underline{H}^c-\underline{\Delta}^c]^{-1} , \tag{3.18}$$

where H^c is the intracluster part of the Hamiltonian, Eq. (2.1), and $\underline{\Delta}^c$ is the cluster renormalized interactor describing the effect of the surrounding medium on the cluster c. Since by definition $\underline{\Delta}^c$ is independent of the occupation of the sites in the cluster, it can easily be determined within successive levels of approximation from Eq. (3.18) through a replacement of $\underline{H}^c$ by the corresponding part, $\bar{H}^c$, of an effective medium Hamiltonian. Thus, we obtain

$$\underline{\Delta}^c=z\underline{I}-\bar{\underline{H}}^c-[\bar{\underline{G}}^c]^{-1} , \tag{3.19}$$

where the site matrix elements of $\bar{\underline{G}}^c$ are determined from Eq. (3.10). Once $\underline{G}^c$ has been evaluated, one obtains local densities of states associated with any site i and any cluster configuration J through the simple generalization of Eq. (3.3),

$$n_i^J(E)=-\frac{1}{\pi}\mathrm{Im}G_{ii}^{c,J}(E) \ . \tag{3.20}$$

IV. NUMERICAL RESULTS

We have used both the exact algorithm presented in Sec. II and the surface generalization of the CPA and the ECM summarized in Sec. III to calculate the DOS on the surface of random substitutionally disordered semi-infinite alloys based on a square lattice, cf. Fig. 1. In all cases, the values of the alloy parameters chosen in the calculations are stated in the figure captions. Figure 2 shows the exact DOS's obtained through the application of the exact algorithm of Sec. II to samples with 30×30, 100×100, and 100×500 sites. The DOS's shown are typical for states on the surface corresponding to the "central" site along an edge of the sample, cf. site C_0 in Fig. 1.

As is seen in Fig. 2(a) the DOS corresponding to the relatively small sample, 30×30, shows a great deal of structure and is asymmetric about the center of the band, $E=0$. Increasing the size of the sample to 100×100 sites [Fig. 2(b)] and to 100×500 sites [Fig. 2(c)] reduces the structure substantially and produces DOS spectra with the proper symmetry in energy. Thus, the numerical algo-

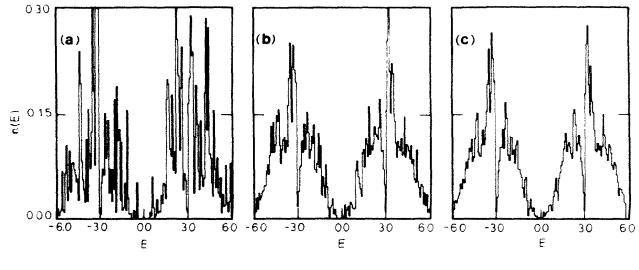

FIG. 2. Exact DOS's for semi-infinite alloys on a square lattice, associated with samples of (a) 30×30, (b) 100×100, and (c) 100×500 sites, panels left to right, respectively. Here, $\varepsilon_A=-\varepsilon_B=3.0$, $W=1.0$, and $C=0.5$.

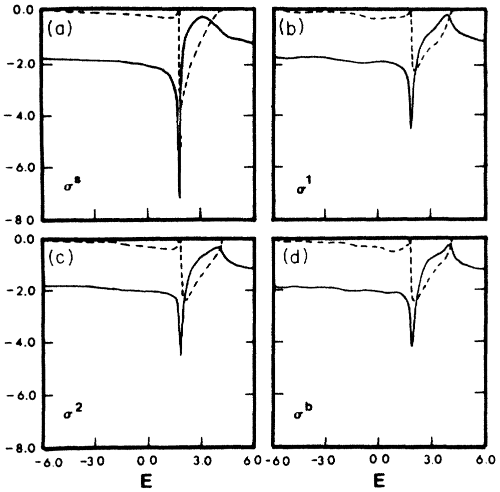

FIG. 3. Real (solid curve) and imaginary part (dashed curve) of the self-energy in a three-plane $I_{\max}=2$ application of the CPA to the semi-infinite alloy with parameters $\varepsilon_A=-\varepsilon_B=2.0$, $W=1.0$, and $\varepsilon=0.10$ for (a) σ^s; (b) σ^1; (c) σ^2; and (d) σ^b.

rithm yields spectra which properly satisfy the "self-averaging" property, i.e., becoming stable with increasing sample size and having the proper symmetry and analytic behavior. We note that in this strong scattering case, the exact results show clearly the presence of subbands, "centered" at the values of ε_A and ε_B, associated with the atoms of the two species in the alloy. These features are expected for disordered systems and are analogous to the corresponding results for one-dimensional disordered chains.

Results for the self-energies obtained in a three-plane CPA calculation, $I_{\max}=2$ are shown in Fig. 3. The figure depicts the real and imaginary parts of the self-energies associated with the surface plane, the first and second planes below the surface as well as the planes in the bulk of the material. In this case, the self-energy was restricted to the same value for all planes below the second. As is seen in Fig. 3 the self-energy, as a local quantity, indeed converges quite rapidly with increased distance from the surface. In fact, the "bulk" self-energy, σ^b, is practically identical to that obtained in an independent application of the CPA to an infinite two-dimensional bulk alloy. This is in keeping with previous results,[8] and justifies the truncation of the set of Eqs. (3.12) at a relatively small value of $I_{\max}$.

In contrast to the rapid convergence of the CPA self-energy, the site-diagonal Green function, being of a more global character, converges relatively slowly with increasing distance from the surface. It is seen in Fig. 4, that the Green function at the ninth plane below the surface is still different from that of the bulk at low energies. The rate of convergence increases somewhat with increasing concentration, i.e., increasing disorder, but is generally quite more sluggish than that of the self-energy.

Figure 5 depicts the DOS obtained in the CPA (left column) and in the ECM (right column) for two different alloy systems. In each case both the CPA and the ECM clearly exhibit the formation of two subbands associated with the two species of the alloy. As expected, the CPA yields smooth DOS curves which reflect the overall features of the surface DOS. The ECM on the other hand displays considerably more structure exhibiting the effects of local statistical fluctuations. These ECM surface densities of states are obtained at the center of a cluster of six sites, three of which are confined to the surface and three on the plane below the surface, cf. Fig. 1. As is seen in Fig. 5 the introduction of second neighbor (W_2) hopping introduces an asymmetry in the DOS spectra although the overall character of the bands remains similar to that of alloys with hopping confined to nearest neighbors.

The accuracy of the ECM, even with rather small clusters, is exhibited explicitly in Fig. 6. Here, the surface DOS for the center of a cluster of six sites calculated in the ECM is compared with exact spectra obtained using the recursion method. It is seen that the ECM properly reproduces the main peak in the exact DOS and much of the subsidiary structure. The agreement between the exact and analytic (ECM) results would be expected to increase with increasing cluster size used in the application of the ECM.

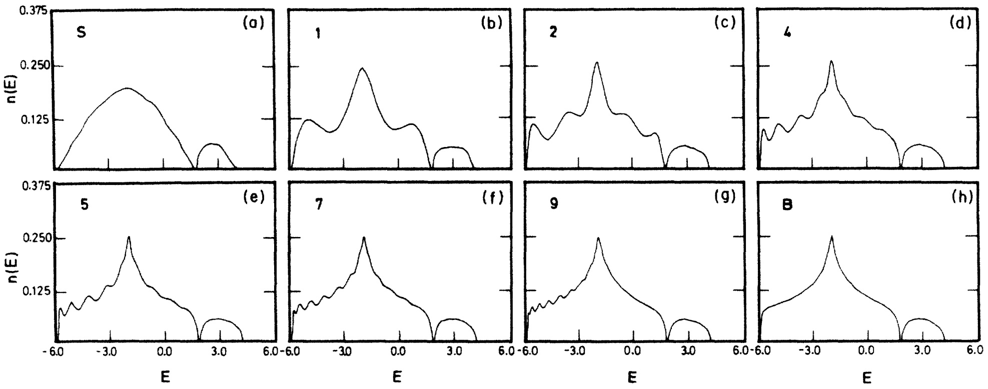

FIG. 4. DOS's at and below the surface of a two-dimensional semi-infinite alloy obtained in the CPA for the alloy characterized in Fig. 3.

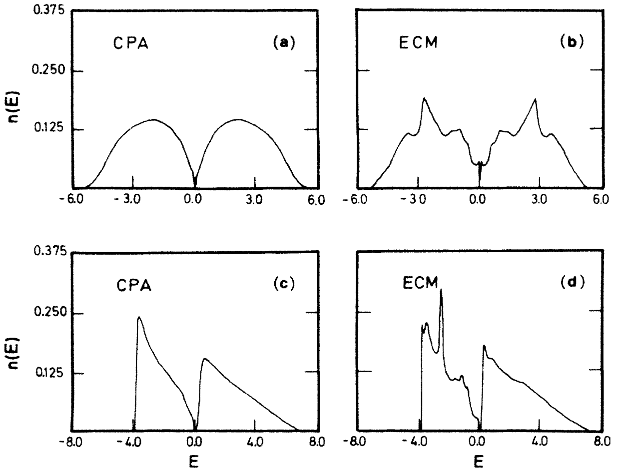

FIG. 5. CPA, left column, and ECM, right column DOS's for two semi-infinite alloy systems on a square lattice. Here, $\varepsilon_A = -\varepsilon_B = 2.0$, and $c = 0.5$ for both alloys, with $W_1 = 1.0$, $W_2 = 0.0$ for the alloy on the top row, panels (a) and (b) and $W_1 = 1.0$, $W_2 = 0.5$ for that in panels (c) and (d).

In addition to providing rather accurate overall DOS's, the ECM can also yield DOS's associated with specific cluster configurations. Several such spectra are exhibited in Fig. 7. These DOS's exhibit the expected structure such as the Slater-Koster impurity peak for an *A*-atom impurity surrounded by *B* atoms [Fig. 7(a)]. On the other hand, partial cluster DOS also bring forth certain limitations imposed by the use of a single-site effective medium. As discussed elsewhere,[43] such a medium in conjunction with the ECM can lead to a particularly poor description of band edges and of partial DOS's associated with large clusters of like atoms. Thus, the configurational DOS for a cluster of atoms of type *A* [Fig. 7(b)] fails to satisfy the integral sum rule by about 15%. By contrast, the DOS in Figs. 7(a) and 7(c) satisfies the sum rule quite accurately (within the numerical accuracy of the calculation). In the absence of a fully self-consistent cluster theory, a way out of this difficulty would be to use a more accurate embedding medium such as that obtained[43] in a "two-site" CPA calculation. In any case, the ECM can be expected to yield correct average DOS's, cf. Fig. 7(c), and in principle allows the introduction of short-range order into the averaging process.

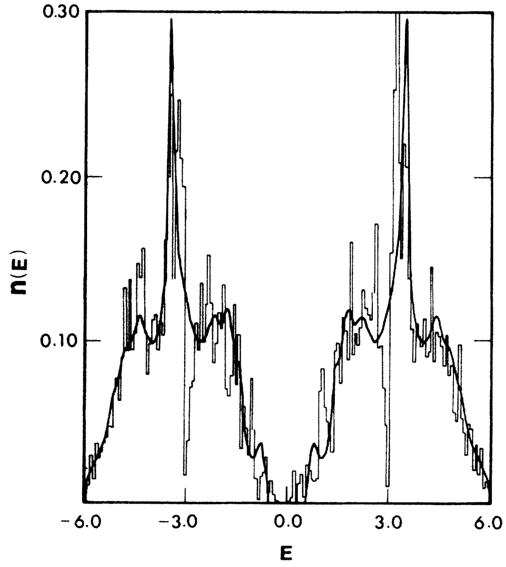

FIG. 6. Comparison of exact (histogram) and ECM (heavy curve), total densities of states for the surface of the semi-infinite square alloy characterized in Fig. 2.

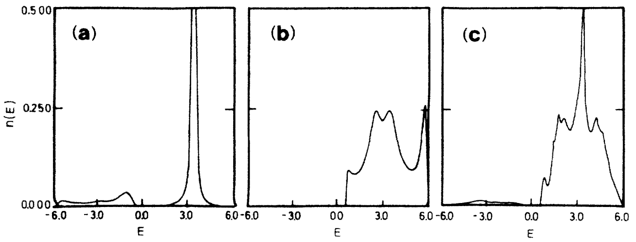

FIG. 7. Configurational DOS's calculated for the alloy in Fig. 6: (a) an *A* atom surrounded by *B* atoms, (b) an *A* atom surrounded by *A* atoms, and (c) the average DOS for an *A* atom over all possible cluster configurations.

V. DISCUSSION AND CONCLUSIONS

We have presented both an exact numerical technique as well as analytic approximations for the calculation of the single-particle Green function on or near the surface of concentrated substitutionally disordered alloys. The numerical algorithm discussed here is computationally feasible with alloys of general dimensionality. This makes the technique preferable to the position-space renormalization-group (decimation) method whose computational complexity increases dramatically with increasing dimension. The results of an application of the method to semi-infinite disordered systems in two dimensions shows that stable results are obtained with samples containing only moderately large numbers of sites (see Fig. 2).

Of the analytic methods discussed here, one is a generalization[8] to the study of surfaces of the CPA for bulk alloys, while the other is an extension of the ECM (Refs. 19 and 20) to the calculation of the DOS at or near the surface of substitutionally disordered systems. Our numerical results reveal that the relative accuracy of these two analytic methods in the calculation of surface DOS's is similar to that in the corresponding calculation of bulk DOS's. In particular, the ECM yields DOS's which properly reflect the structure in the exact spectra and thus accounts for the effects of local statistical fluctuations on the surface of a substitutionally disordered solid.

As mentioned earlier, we neglected all effects of surface relaxation, such as differences in the potentials, concentrations or structure at or near the surface of an alloy. Indeed these effects are expected to be present in realistic systems. From our discussion it follows that the CPA can account for variations in the potentials and concentration in a straightforward way. Short-range structure effects can also be taken into account in a matrix generalization of the scalar method discussed here. Clearly, surface relaxation and the treatment of short-range order effects, not possible within the CPA can be incorporated into a cluster method such as the ECM in quite a simple manner.

We close our discussion with a comment regarding the application of the analytic methods presented here to realistic three-dimensional TB disordered systems. As is well known, most three-dimensional disordered systems usually display rather mild structure as compared with their one-dimensional counterparts. For such systems the single-site CPA can be expected to provide a reliable method of study. On the other hand, the study of short-range order effects and related properties require the use of a multisite (cluster) method. For the treatment of such effects, the ECM in conjunction with even small clusters of atoms (say 2 or 3) can be expected to yield a sufficiently accurate approximation for most purposes.

ACKNOWLEDGMENTS

This work was partly supported by the National Science Foundation (through the Northwestern University Materials Research Center, under Grant No. DMR-82-16972).

---

[1] M. Hwang, R. Podloucky, A. Gonis, and A. J. Freeman, Phys. Rev. B **33**, 765 (1986).

[2] J. B. Pendry, *Low-Energy Electron Diffraction* (Academic, New York, 1974).

[3] G. Koster and J. Slater, Phys. Rev. **95**, 1167 (1954).

[4] D. Kalkstein and P. Soven, Surf. Sci. **26**, 85 (1971).

[5] L. Falicov and F. Yndurain, J. Phys. C **8**, 147 (1975).

[6] D. H. Lee and J. D. Joannopoulos, Phys. Rev. B **17**, 1816 (1978); **23**, 4988 (1981).

[7] J. Pollmann and S. T. Pantelides, Phys. Rev. B **18**, 5524 (1978).

[8] N. F. Berk, Surf. Sci. **48**, 289 (1975).

[9] J. L. Moran-Lopez, G. Kerker, and K. H. Bennemann, Surf. Sci. **57**, 540 (1975); Phys. Rev. B **15**, 638 (1977).

[10] J. Ladik and M. Seel, Phys. Rev. B **13**, 5388 (1976).

[11] J. Ladik, Int. J. Quantum Chem. **23**, 1073 (1983).

[12] R. S. Day and F. Martino, Chem. Phys. Lett. **84**, 86 (1981).

[13] C. E. T. Goncalves da Silva and B. Koiller, Solid State Commun. **40**, 215 (1981).

[14] J. M. Langlois, A. M. S. Trembley, and B. W. Southern, Phys. Rev. B **21**, 218 (1983).

[15] G. Bryant, Phys. Rev. B **31**, 5166 (1985).

[16] R. Haydock, V. Heine, and M. J. Kelly, J. Phys. C **8**, 2591 (1975).

[17] A. Mookerjee, J. Phys. C **6**, L205 (1973); **6**, 1340 (1973); **7**, 4069 (1974); **8**, 2688 (1975).

[18] T. Kaplan and L. J. Gray, Phys. Rev. B **14**, 3462 (1976).

[19] A. Gonis and J. W. Garland, Phys. Rev. B **16**, 2424 (1977).

[20] C. W. Myles and John D. Dow, Phys. Rev. Lett. **42**, 254 (1979); Phys. Rev. B **19**, 4939 (1979).

[21] P. Soven, Phys. Rev. **156**, 809 (1967).

[22] B. Velický, S. Kirpatrick, and H. Ehrenreich, Phys. Rev. **175**, 747 (1968).

[23] F. Yonezawa and K. Morigaki, Prog. Theor. Phys. Suppl. **53**, 1 (1973).

[24] R. J. Elliott, J. A. Krumhansl, and P. L. Leath, Rev. Mod. Phys. **46**, 465 (1974).

[25] B. L. Györffy and G. M. Stocks, in *Electrons in Disordered Metals and Metallic Surfaces,* edited by P. Phariseau, B. L. Györffy, and L. Scheire (Plenum, New York, 1978), p. 89, and references therein.

[26] J. S. Faulkner, in *Progress in Material Science,* edited by J. W. Christian, P. Hassen, and T. B. Massalski (Pergamon, New York, 1982), Vols. 1 and 2, and references therein.

[27] E. Müller-Hartmann, Solid State Commun. **12**, 1269 (1973).

[28] M. Tsukada, J. Phys. Soc. Jpn. **32**, 1475 (1972).

[29] Z. Zittartz, Solid State Commun. **14**, 51 (1973); Z. Phys. **267**, 245 (1974).

[30] F. Ducastelle, J. Phys. F **2**, 468 (1972).

[31] F. Brauers, F. Ducastelle, F. Gautier, and J. Van der Rest, J. Phys. F **3**, 2120 (1973).

[32] W. H. Butler, Phys. Rev. Lett. **39A**, 203 (1972).

[33] B. G. Nickel and W. H. Butler, Phys. Rev. Lett. **30**, 373 (1973).

[34] W. H. Butler, Phys. Rev. B **8**, 4499 (1973).

[35] P. Lloyd and P. R. Best, J. Phys. C **8**, 3752 (1975).

[36] N. F. Berk and R. A. Tahir-Kheli, Physica (Utrecht) **67**, 501 (1973).

[37] R. Mills and P. Ratanavararaksa, Phys. Rev. B **18**, 5291 (1978).

[38] L. J. Gray and T. Kaplan, Phys. Rev. B **24**, 1872 (1981).

[39] C. Pisani, Phys. Rev. B **30**, 6841 (1984).

[40] M. Hwang, A. Gonis, and A. J. Freeman, Phys. Rev. B **33**, 2872 (1986).

[41] P. Dean, Rev. Mod. Phys. **44**, 127 (1972).

[42] The algorithm was proposed by A. Mackinnon [J. Phys. C **13**, L131 (1980)] to investigate the localization properties of the one-dimensional Anderson model. In this paper, we adapt the method to calculate the densities of states of a finite-size disordered system.

[43] A. Gonis and A. J. Freeman, Phys. Rev. B **29**, 4277 (1984).